

# Histological Evidence of Mucosal Barrier in Small Intestine of the Bullfrog (*Lithobates catesbeianus*)

Evidencia Histológica de la Barrera Mucosa en el Intestino Delgado de la Rana Toro (*Lithobates catesbeianus*)

Wenjun You<sup>1</sup>; Hao Li<sup>1</sup>; Honghua Chen<sup>1</sup>; Xiaoshu Zhan<sup>1</sup>; Canying Liu<sup>1</sup>; Shengfeng Chen<sup>1</sup>; Yaqiong Ye<sup>1</sup> & Hui Zhang<sup>1,2</sup>

YOU, W.; LI, H.; CHEN, H.; ZHAN, X.; LIU, C.; CHEN, S.; YE, Y. & ZHANG, H. Histological evidence of mucosal barrier in small intestine of the bullfrog (*Lithobates catesbeianus*). *Int. J. Morphol.*, 44(1):60-70, 2026.

**SUMMARY:** The small intestine mucosa represents a critical barrier between the inner and outer environment. Although the organization of the intestinal mucosal barrier has been extensively studied in mammals, data from non-mammalian vertebrates remain limited. Here we characterized the mucosal barrier organization in small intestine of the bullfrog (*Lithobates catesbeianus*) through histological and ultrastructural analyses. Histological investigation showed that small intestinal wall of the *L. catesbeianus* was thin due to small number of smooth muscle cell layers in the muscularis mucosae (thickness  $1.82 \pm 0.32 \mu\text{m}$ ) and muscularis (thickness  $44.95 \pm 3.22 \mu\text{m}$ ). Transmission electron microscopy (TEM) investigation showed the junctional complexes including tight junctions between enterocytes, and the shedding extracellular vesicles were observed in close proximity to the surface of microvilli in the lumen. These structures formed a physical barrier together with the epithelial cells and the mucus layer. In addition, a relatively elementary immune barrier was composed of mucosal resident immune cell types, including lymphocytes, macrophages, mast cells, plasma cells, eosinophils and enteroendocrine cells. Taken together, the mucosal barrier of small intestine in the *L. catesbeianus* consisted of two parts, physical barrier and immune barrier, which constituted a relatively well-developed small intestine mucosal barrier of *L. catesbeianus*. These findings provide baseline data for understanding mucosal barrier evolution in vertebrates.

**KEY WORDS:** Amphibian; Intestine; Ultrastructure; Immune.

## INTRODUCTION

In vertebrates, the mucosa lines the intestine, urogenital tracts, respiratory airways, epithelia of exocrine glands, eye conjunctiva, and inner ear (Dwivedy & Aich, 2011). Of these mucosal types, the small intestinal mucosa has the largest area of coverage, and it is exposed to a mixture of undigested and digested food, secreted gastric acid and bile acids, bacterial components and metabolites, and damage-associated molecular patterns (Akiba *et al.*, 2020). As such, small intestine mucosa represents one of the body's most critical interfaces with the external environment.

Beyond its primary role in nutrient absorption, the small intestinal mucosa functions as a selective barrier, protecting against the vast amount of commensal and pathogenic microbes and potentially immunogenic macromolecules (Peterson & Artis, 2014). Under normal physiological conditions, the mucosal barrier allows small amounts of antigens to pass the mucosa to interact with the

innate and adaptive immune systems, and it is the main defense line to against potentially harmful substances and infectious agents (An *et al.*, 2022). However, disruption of mucosal barrier regulation can lead to increased antigen and bacterial translocation, resulting in mucosal damage and subsequent pathological conditions (Keita & Söderholm, 2010). Thus, small intestine mucosal barrier plays a pivotal role in regulating intestinal permeability, detecting and eliminating the pathogenic microbial debris, and maintaining intestinal homeostasis (Peterson & Artis, 2014).

Amphibians, as evolutionarily ancestral vertebrates, have emerged as valuable animal models for comparative and developmental studies of immunity (Yaparla *et al.*, 2017). While extensive research on the small intestinal mucosal barrier has been conducted in mammalian models, data from lower vertebrates — particularly amphibians — remain scarce. The cellular mechanisms underlying

<sup>1</sup> College of Animal Science and Technology, Foshan University, Foshan, China.

<sup>2</sup> College of Animal Science and Technology, Jiangxi Agricultural University, Nanchang, China.

FUNDING. This work was supported by the National Natural Science Foundation of China (No. 31760716 and 31560681).

amphibian intestinal mucosal barrier function are still poorly understood. Currently, amphibian populations worldwide are facing alarming declines due to multifaceted threats, including habitat destruction, climate change, pollution, and increasingly prevalent bacterial, fungal, and viral infections (Valencia-Aguilar *et al.*, 2015; Oliveira *et al.*, 2023). These compounding stressors likely impair amphibian immune competence, reducing their ability to mount effective defenses and leading to elevated mortality rates (Yaparla *et al.*, 2017). To mitigate this decline, a critical first step is to characterize the immunological barriers that pathogens must overcome during infection.

The American bullfrog (*Lithobates catesbeianus*), a widely distributed anuran amphibian native to North America and introduced globally, represents an experimental model for biological studies in the fields of pharmacology, medicine, and reproduction biology (Segatelli *et al.*, 2009). Moreover, *L. catesbeianus* are also commercially farmed worldwide as an economic animal on a large scale. In this study, we investigate the structural and functional components of small intestinal mucosal barrier — the largest immune interface in the *L. catesbeianus*. Our findings will provide essential histological insights to support the development of mucosal immunity-based vaccines and conservation strategies for amphibian species.

## MATERIAL AND METHOD

### Animals and tissues

One hundred and sixty-day-old cultured *L. catesbeianus*, obtained commercially from an aquaculture farm, were used in this study. Six specimens were anesthetized on ice to induce torpor (4 °C for 30 min) and subsequently euthanized via rapid spinal cord disruption, in accordance with international animal welfare guidelines. Every effort was made to minimize animal suffering throughout the procedure. Small intestinal segments were excised, luminal contents were flushed with 0.9 % physiological saline, and tissue samples were immediately fixed in either Bouin's solution for light microscopy or 2.5 % glutaraldehyde/PBS for transmission electron microscopy (TEM) analysis.

### Histology by hematoxylin and eosin (H&E) staining

Small intestinal segments were fixed in Bouin's solution and subsequently processed through a graded ethanol series (70 % to 100 %) for dehydration. Following dehydration, tissues were paraffin-embedded and sectioned at 5  $\mu$ m thickness using a microtome (Leica, Germany). After xylene-mediated dewaxing, sections were stained with hematoxylin and eosin (H&E). Stained sections were coverslipped and

examined under a light microscopy (Nanjing, China), with digital photomicrographs captured using Scope Image 9.0 (H3D) software.

### Transmission electron microscopy (TEM)

Ultrastructural analysis was performed by TEM following established protocols (Ge *et al.*, 2019). Small intestinal samples were immediately fixed in 2.5 % glutaraldehyde in 0.1 M PBS (pH 7.4) at 4 °C for 48 h. After primary fixation, specimens were post-fixed in 1 % osmium tetroxide ( $\text{OsO}_4$ ) for 1 h at room temperature, then dehydrated through a graded ethanol series (70-100 %). Tissues were subsequently infiltrated with propylene oxide/Araldite resin mixture and embedded in pure Araldite. Ultrathin sections (70-90 nm) were collected on copper grids and double-stained with 1 % uranyl acetate followed by Reynold's lead citrate, each for 20 min. Sections were examined using a H-7650 TEM (Hitachi, Japan) equipped with a high-resolution digital imaging system.

### Morphometrical analysis

Morphometric analysis was conducted following established protocols (Wang *et al.*, 2024) using ImageJ (FiJi) software (NIH, USA). The following parameters were quantified: (i) thickness of small intestinal wall layers, (ii) microvillar dimensions (height and width), (iii) cellular and intracellular granule diameters, and (iv) extracellular vesicle diameters.

For measurement procedures: (i) micrographs were imported into ImageJ and calibrated using the "Set Scale" function (Analyze menu) according to each image's original scale bar, converting pixel units to micrometers ( $\mu$ m), (ii) linear measurements were obtained using the "Straight Line" tool, with values recorded via the "Measure" function (Analyze menu), and (iii) all data were processed using Microsoft Excel (Microsoft, USA) and expressed as mean  $\pm$  standard deviation.

## RESULTS

### Microstructure of the wall in small intestine of *L. catesbeianus*

The small intestine was a hollow tubular structure, consisting of a central lumen surrounded by a wall composed of four main layers: mucosa, submucosa, muscularis, and serosa (Fig. 1). The thicknesses of these layers were measured and were presented in Table I. Finger-like villi were clearly visible in the small intestine (Fig. 1a), with an average length of  $247.96 \pm 73.57 \mu$ m (Table I). In contrast, the intestinal crypts (crypts of Lieberkühn) were not observed (Fig. 1a, 1b).

Table I. Morphological parameters of small intestine in the *L. catesbeianus*.

Items	Mean±SD (μm)
Thickness of mucosa	34.60 ± 1.50
Thickness of lamina propria	7.86 ± 1.05
Thickness of muscularis mucosae	1.82 ± 0.32
Thickness of submucosa	28.47 ± 4.28
Thickness of muscularis	44.95 ± 3.22
Thickness of inner circular muscle layer of muscularis	36.22 ± 2.12
Thickness of outer longitudinal muscle layer of muscularis	8.67 ± 1.46
Thickness of serosa	6.51 ± 1.33
Length of villus	247.96 ± 73.57
Width of villus	76.34 ± 2.50
Height of epithelium	29.31 ± 3.79
Length of microvilli	1.68 ± 0.17
Width of microvilli	0.10 ± 0.01

The small intestine mucosa was composed of the three layers: epithelium, lamina propria, and muscularis mucosae (Fig. 1). Their thicknesses were also measured (Table I). The simple columnar epithelium covering the villi and the surface of the intervillar spaces was composed of surface absorptive enterocytes and goblet cells (Fig. 1). In the epithelium, the predominating absorptive enterocytes were interspersed with goblet

cells. The intraepithelial lymphocytes were also observed (Fig. 1b, 1c). The enterocytes were tall columnar cells exhibiting oval, basally located nuclei. At the apex of each enterocyte was a layer of densely packed microvilli. Abundant microvilli at the cell apex were seen to form the striated border (Fig. 1c).

The loose connective tissue of the lamina propria formed the core of the villi, which liked trees of a forest rise above the surface of the small intestine. The remainder of the lamina propria, which extended down to the muscularis mucosae, was composed of 1-2 circular layers of smooth muscle cells. (Fig. 1a, 1b). The thickness of muscularis mucosae was  $1.82 \pm 0.32 \mu\text{m}$  (Table I). The outer longitudinal layers of smooth muscle cells were not observed in the

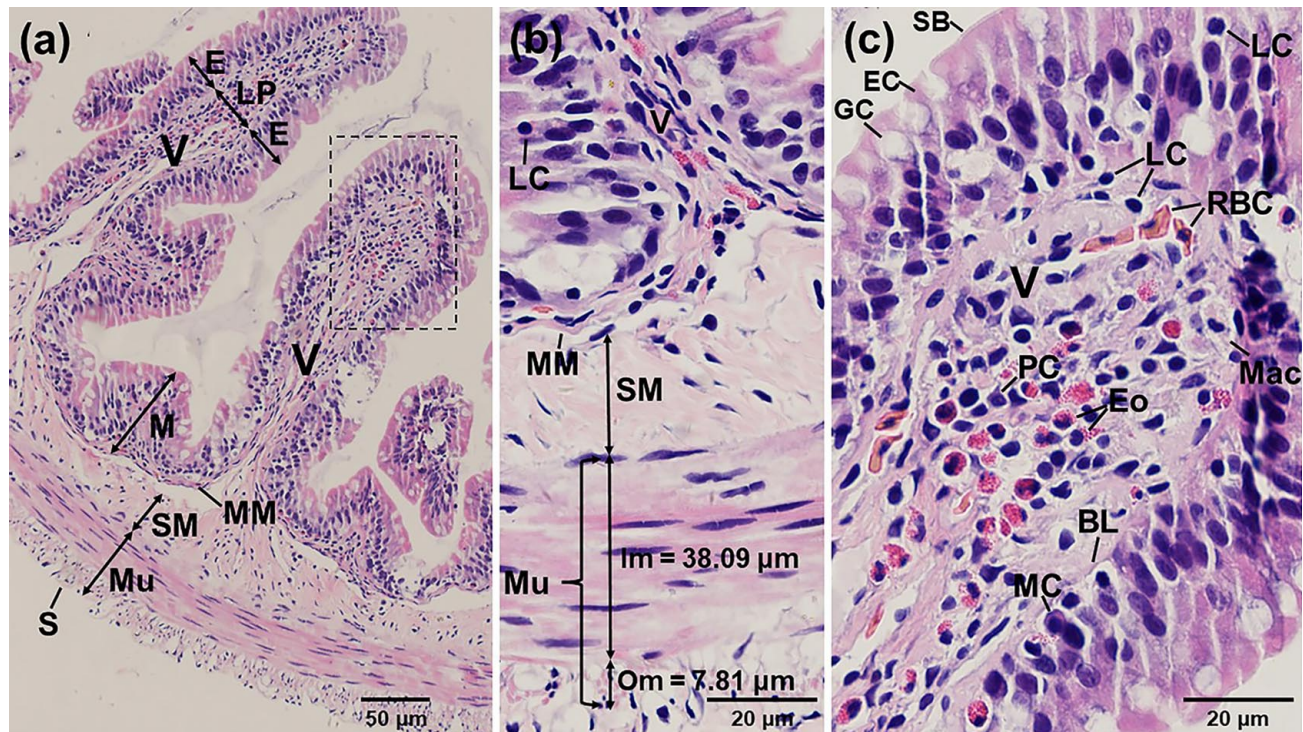


Fig. 1. Light micrographs of small intestine wall in the bullfrog by H&E staining. (a) The transverse section of the small intestine. The small intestine wall is composed of mucosa (M), submucosa (SM), muscularis (Mu) and serosa (S). Many small intestine villi (V) are observed to extend into the intestinal lumen. E, epithelium; MM, muscularis mucosae; LP, lamina propria. (b) High magnification micrograph with details of small intestine wall. The Mu consists of inner circular muscle layer (Im) and outer longitudinal muscle layer (Om). The intraepithelial lymphocytes (LC) are observed. SM, submucosa; V, intestinal villi; MM, muscularis mucosae. (c) High magnification micrograph of the black dashed line boxed area shown in (a) with details of cell types in the epithelium and lamina propria. The cell types of the epithelium of mucosa consist of enterocytes (EC), goblet cells (GC) and intraepithelial lymphocytes (LC). In the lamina propria, the stromal cell types, including lymphocytes (LC), macrophages (Mac), and eosinophils (Eo), plasma cells (PC) and mast cells (MC) are observed. SB, striated border; RBC, red blood cell. BL, basal lamina.

muscularis mucosae. Notably, the lamina propria was rich in immune cell types, including lymphocytes, macrophages, eosinophils, mast cells and plasma cells (Fig. 1).

The submucosa of the small intestine consisted of dense, irregular fibroelastic connective tissue. The Brunner's glands were not observed in the submucosa. The muscularis contained smooth muscle cells that were spirally oriented and divided into two sublayers according to the main direction the muscle cells follow, that was inner circular muscle layer and outer longitudinal muscle layer (Fig. 1a, 1b). Their thickness was approximately  $36.22 \pm 2.12 \mu\text{m}$  and  $8.67 \pm 1.46 \mu\text{m}$ , respectively. The inner circular muscle layer was thicker than outer longitudinal muscle layer. The serosa was a thin layer of loose connective tissue with blood vessels and adipose tissue (Fig. 1a, 1b).

#### Ultrastructure of the epithelium and the physical barrier in small intestine of *L. catesbeianus*

The epithelium of mucosa was comprised of absorptive enterocytes and goblet cells (Fig. 2a). Goblet cells were interspersed between the absorptive enterocytes.

The polygonal and electron lucent mucinogen granules were located in the apex of goblet cells. The mucinogen granules were  $1.13 \pm 0.23 \mu\text{m}$  in diameter (Table II). Goblet cells had no microvilli. Each enterocyte was tall columnar cell with an oval nucleus in the basal half of the cell (Figs. 2 and 3). The apical surface of each enterocyte was a homogeneous layer - striated border, which was seen to be a layer of densely packed microvilli. Each microvillus was a cylindrical protrusion of the apical cytoplasm that was  $1.68 \pm 0.17 \mu\text{m}$  tall by  $0.10 \pm 0.01 \mu\text{m}$  in diameter (Table I). The cytoplasm of enterocytes was rich in mitochondria. Moreover, electron lucent vesicles, multivesicular bodies and electron dense absorptive granules were observed in the plasma of enterocytes (Fig. 3a).

The lysosomes with various developmental stages according to their electron density were also observed (Fig. 2b). They were approximately  $3.24 \mu\text{m}$  in diameter. The shedding extracellular vesicles were observed in close proximity to the surface of microvilli in the lumen (Fig. 3b). The shedding vesicles were  $0.13 \pm 0.04 \mu\text{m}$  in diameter (Table II). The lateral cell membranes of two adjacent enterocytes formed junctional complexes, which including tight junctions, adherens junctions and desmosomes (Fig. 3). In particular, the desmosomes were frequently observed

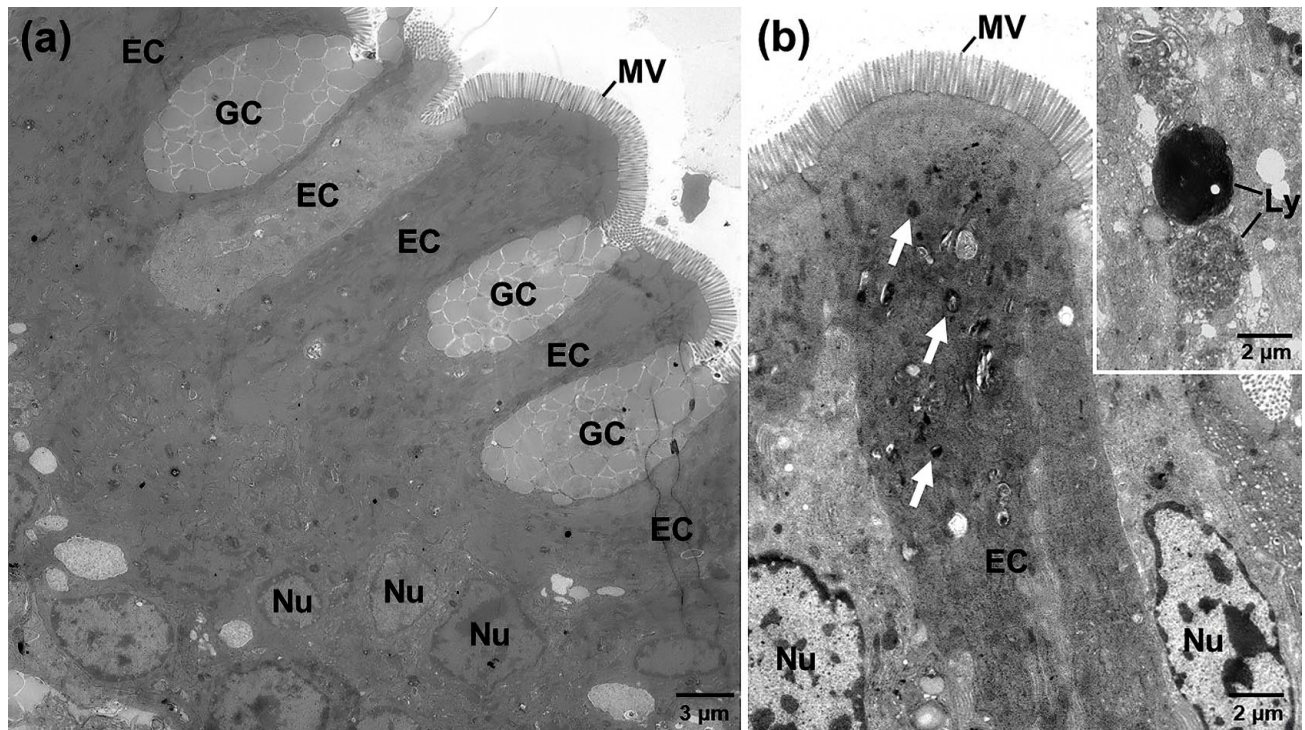


Fig. 2. TEM micrographs of epithelium in the small intestine of the bullfrog. (a) The enterocytes (EC) and goblet cells (GC) are located alternately to constitute the epithelium of the mucosa. GC characterized by apical cytoplasm filled with mucous granules are present among the EC. The EC are columnar with many microvilli (MV) in the free surface. The GC contain many electron lucent mucinogen granules at the apical region of the cytoplasm. Nu, nucleus. (b) A columnar enterocyte (EC) contains absorptive granules (white arrows). Insert: lysosomes (Ly) with various developmental stages in the plasma of EC. Nu, nucleus.

Table II Diameters of the granules/vesicles in various cell types of small intestine of *Rana catesbeiana*.

Granules/vesicles	Electron density	Diameter ( $\mu\text{m}$ )
Type I granules of eosinophil	An electron-dense internum and a less electron-dense externum	$1.15 \pm 0.24$
Type II granules of eosinophil	An electron-dense internum and an electron-lucent externum	$0.69 \pm 0.12$
Granules of goblet cell	Electron-lucent	$1.13 \pm 0.23$
Granules of mast cell	Electron dense	$1.25 \pm 0.17$
Granules of enteroendocrine cell	Electron dense	$0.11 \pm 0.02$
Granules of nerve fiber	Electron medium	$0.06 \pm 0.01$
Extravillous shedding vesicles	Electron-lucent	$0.13 \pm 0.04$

in midlateral and basolateral membrane domains. The junctional complexes, together with the epithelial cells and the mucus layer, constituted the physical barrier of the small intestine of *L. catesbeianus*.

#### Ultrastructure of cell types in lamina propria and immune barrier in small intestine of *L. catesbeianus*.

In the lamina propria of small intestine, the eosinophils were observed between collagenous fibers of connective tissue (Fig. 4). The eosinophils had a sausage-shaped, bilobed nucleus in which the two lobes were connected by a thin chromatin strand and surrounding

nuclear envelope. The eosinophils contained many specific cytoplasmic granules, which has an electron dense central crystalloid core, the internum, surrounding by a less electron dense externum. The specific granules included rounded and electron dense type I granules ( $G_1$ ), which including a crystal core with a higher electron dense (Fig. 4a). The diameter of type I granules was about  $1.15 \pm 0.24 \mu\text{m}$  (Table II). There were also some eosinophils contained the other type II granules ( $G_2$ ), which were polygonal and electron lucent, also had a crystal core with a higher electron dense (Fig. 4b). The diameter of type II granules was about  $0.69 \pm 0.12 \mu\text{m}$  (Table II). Moreover, lobes of nucleus of the eosinophils were observed (Fig. 4b).

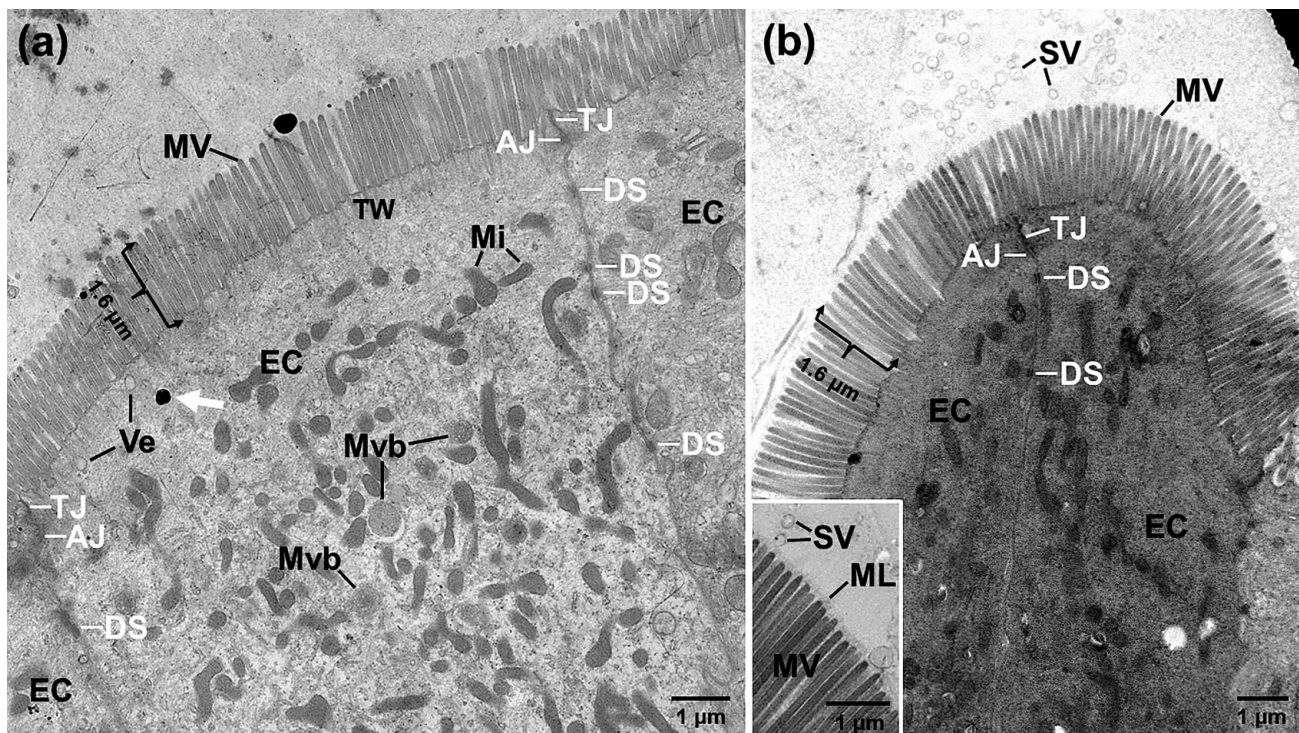


Fig. 3. TEM micrographs of enterocytes (EC) in the small intestine of the bullfrog. (a) The accumulation of mitochondria (Mi) in the apex of EC. The luminal surface is covered with microvilli (MV). The vesicle (Ve), multivesicular bodies (Mvb) and electron dense absorptive granules (white arrows) are observed in the plasma of EC. The junctional complexes, including tight junctions (TJ), adherens junctions (AJ) and desmosomes (DS), are observed between two EC. TW, terminal web. (b) Many shedding vesicles (SV) are observed in close proximity to the surface of MV in the lumen. The junctional complexes are also observed between EC. Insert: The free surface of the microvilli (MV) is covered by a mucus layer (ML). SV, shedding vesicle.

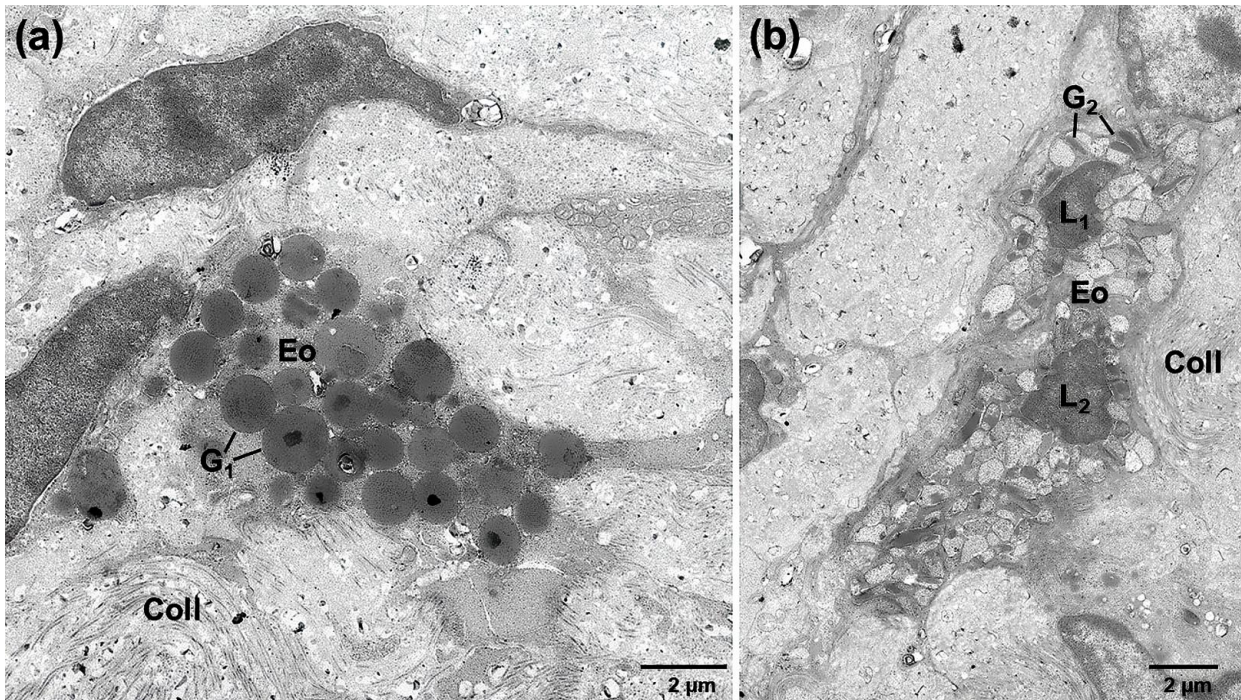


Fig. 4. TEM micrographs of lamina propria of mucosa in the small intestine of the bullfrog. (a) An eosinophil (Eo) with electron dense granules ( $G_1$ ), every granule is rounded and has a crystal core with a higher electron dense. Coll, collagenous fiber. (b) Another eosinophil (Eo) is observed. The eosinophil contains many polygonal electron lucent granules ( $G_2$ ), but every granule has a crystal core with a higher electron dense. The eosinophil has a nucleus with two lobes ( $L_1$  and  $L_2$ ).

Notably, immune cells, including lymphocytes, macrophages, mast cells and plasma cells were also observed

in the lamina propria (Figs. 5 and 6). The lymphocytes had a slightly indented, round nucleus that occupies most of the

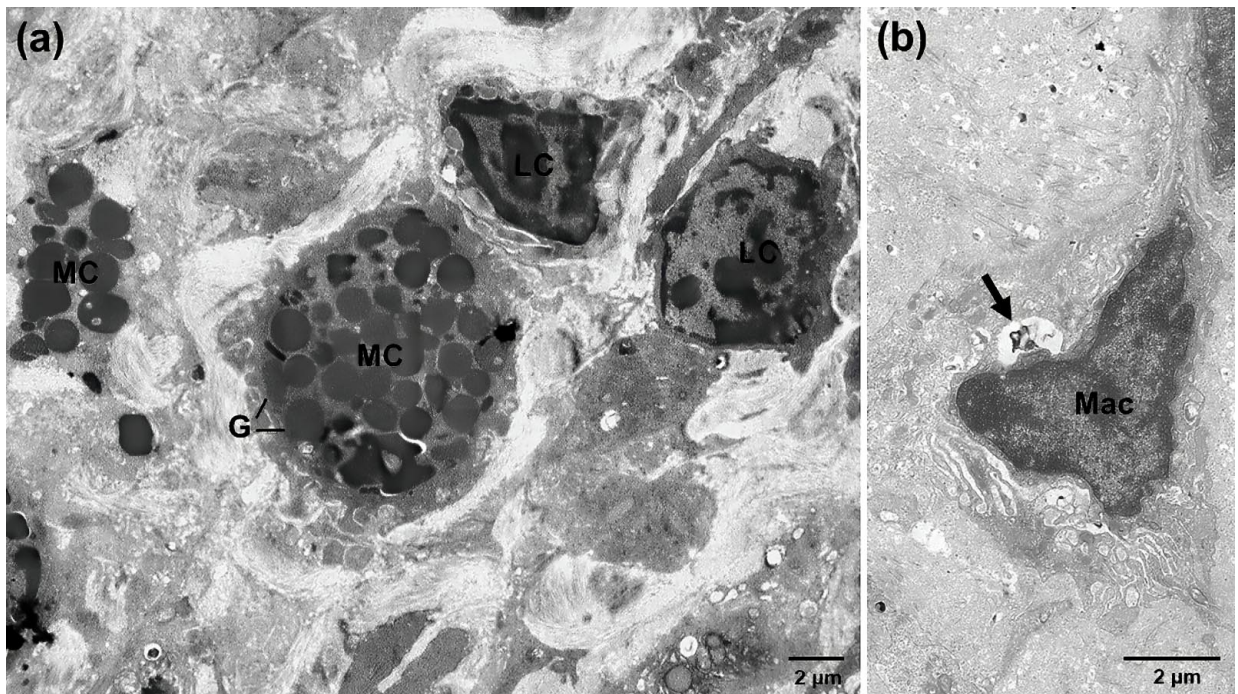


Fig. 5. TEM micrographs of lamina propria of mucosa in the small intestine of the bullfrog. (a) Two mast cells (MC) with rounded and electron dense granules (G). Two lymphocytes (LC) with big nuclei. (b) A macrophage irregular appearance. A residual body (black arrow) in the cytoplasm.

cell (Fig. 5a). The nucleus was dense, rich in heterochromatin, and was acentrically located. The cytoplasm was scarce. Rounded mast cells were larger in size (Fig. 5a). They were approximately 10.46  $\mu\text{m}$  in

diameter. The mast cells contained many rounded and electron dense secretory granules in their cytoplasm. The diameter of secretory granules in the mast cells was about  $1.25 \pm 0.17 \mu\text{m}$  (Table II).

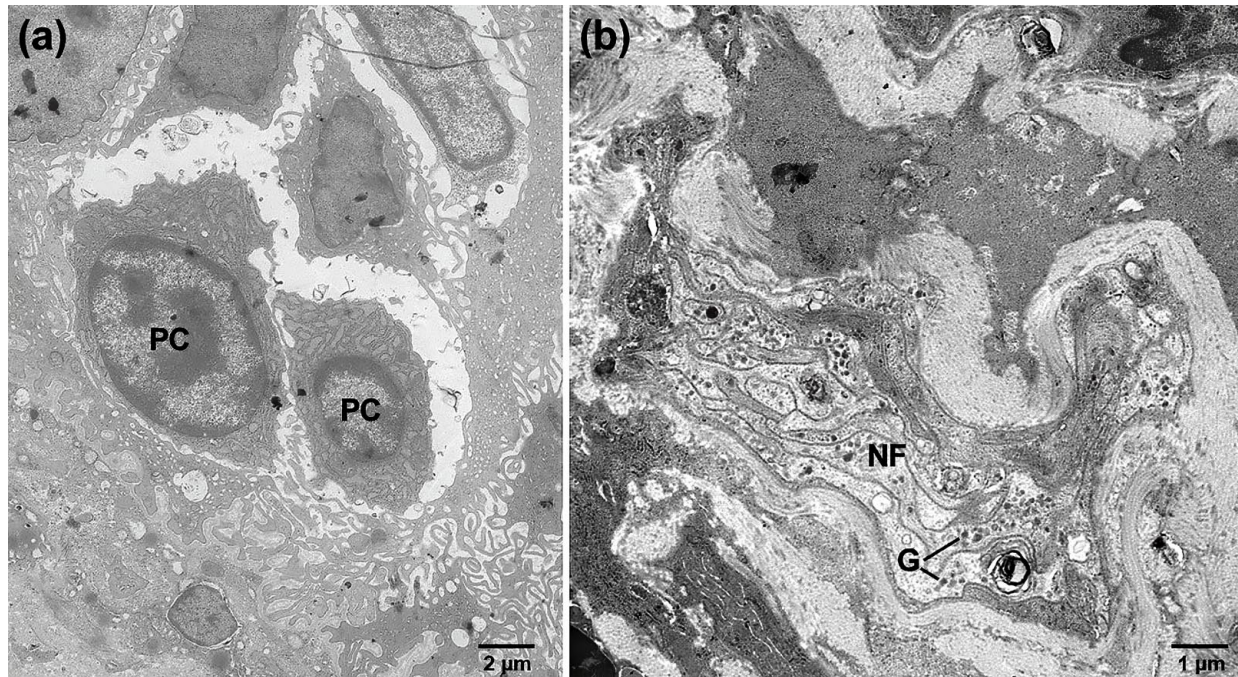


Fig. 6. TEM micrographs of lamina propria of mucosa in the small intestine of the bullfrog. (a) The plasma cells (PC) are observed. Every plasma cell has a rounded nucleus and is biased to one side. The accumulation of endoplasmic reticulum in the cytoplasm of plasma cells. (b) The nerve fibers (NF) with many secretory granules (G) in the lamina propria.

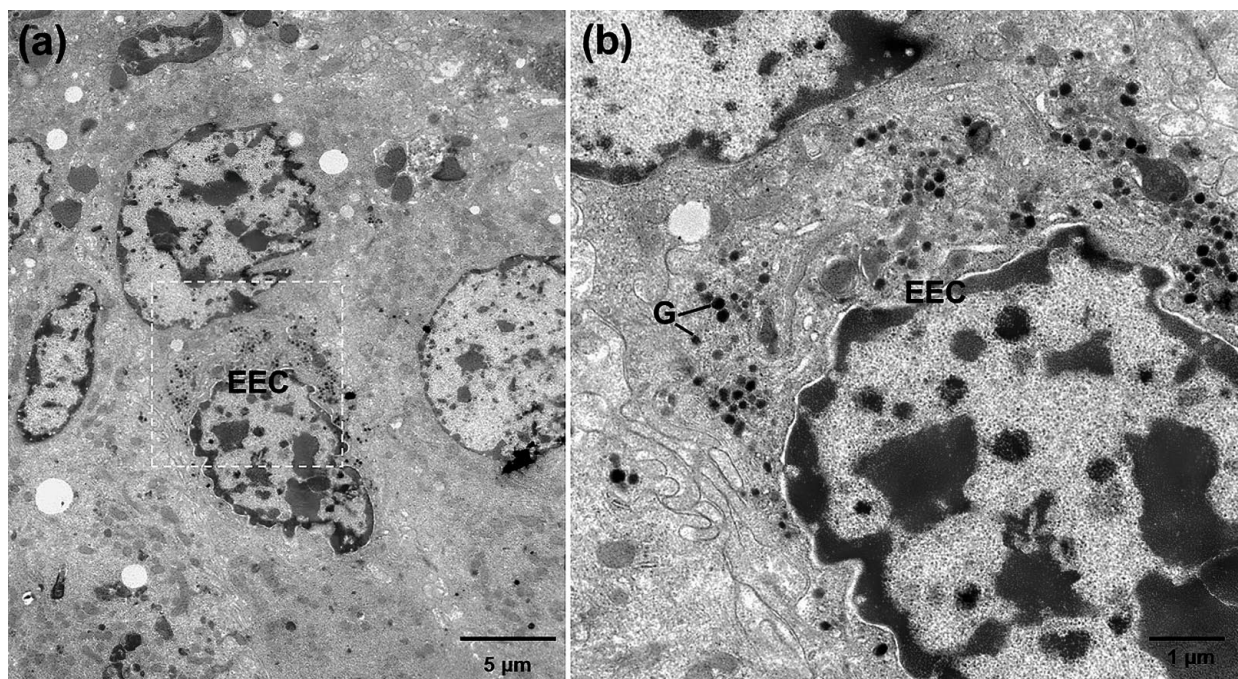


Fig. 7. TEM micrographs of lamina propria of mucosa in the small intestine of the bullfrog. (a) An enteroendocrine cell (EEC) with many rounded and electron dense granules in its cytoplasm. (b) High magnification micrograph of the white dashed line boxed area shown in (a) with details of the cytoplasm and the granules (G) of EEC.

Macrophages were irregularly shaped (Fig. 5b). Their cell surface was uneven, varying from short, blunt projections to finger-like some cytoplasmic processes, filopodia. Their cytoplasm contained many small vacuoles. The residual bodies were clearly observed in the cytoplasm of the macrophages. The plasma cells were observed between fibroblasts in the connective tissue of lamina propria (Fig. 6a). Plasma cells were large with an eccentrically placed nucleus. Their cytoplasm was full of well-developed rough endoplasmic reticula with closely spaced cisternae. The nerve fibers with electron medium granules were also observed (Fig. 6b). The diameter of secretory granules of nerve fibers was about  $0.06 \pm 0.01 \mu\text{m}$  (Table II).

In addition, the enteroendocrine cells with many small, rounded and electron dense secretory granules were observed (Fig. 7). The enteroendocrine cells were closed type, and their secretory granules were found predominantly located on one side of the cell. The secretory granules were about  $0.11 \pm 0.02 \mu\text{m}$  in diameter (Table II). The diffuse immune cells within the lamina propria, together with the intraepithelial lymphocytes, collectively constituted the immune barrier of the small intestine of *L. catesbeianus*. A schematic diagram constituting the structures and cytotypes of the small intestine mucosal barrier in the bullfrog was drawn (Fig. 8).

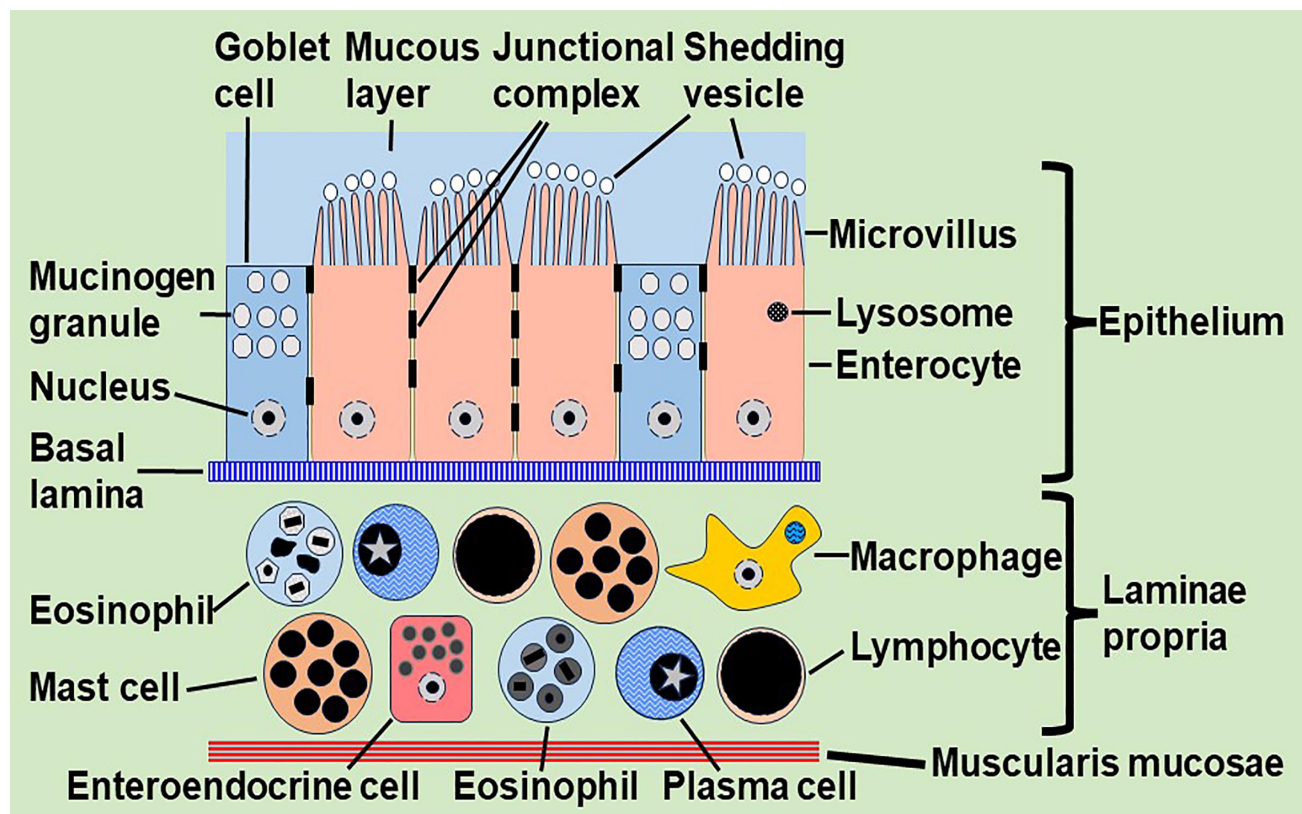


Fig. 8. A schematic diagram illustrating the structure and cell types of small intestine mucosal barrier in the bullfrog.

## DISCUSSION

While the general architecture of the digestive tract wall in amphibians has been documented in previous studies (Bodegas *et al.*, 1997; Bizjak Mali & Bulog, 2004), the ultrastructural characteristics of constituent cell types remain poorly characterized compared to their mammalian counterparts. Although amphibian digestive tract histology shares fundamental similarities with mammals, significant morphological differences exist in small intestinal organization between these vertebrate classes (Bodegas *et al.*, 1997).

In the present study, firstly, the small intestine of *L. catesbeianus* had a thinner wall since the outer longitudinal muscle layer of muscularis was very thin (approximately  $7.81 \mu\text{m}$ ). Moreover, the outer longitudinal layers of smooth muscle cells were not observed in the muscularis mucosae. The muscularis mucosae composed of only 2 layers of smooth muscle cells was also very thin. Therefore, muscularis and muscularis mucosae of small intestine wall of *L. catesbeianus* were not well-developed. Secondly, in contrast the mammalian system, the intestinal crypts between the villi were not

observed in small intestine wall of *L. catesbeianus*. Moreover, the duodenal submucosal glands (Brunner's glands) were also not observed in the submucosa. Thirdly, in the wall of small intestine, although the free lymphocytes were observed between intestinal epithelial cells and other immune cell types were also located in the lamina propria, the aggregated lymphoid nodules (Peyer's patches) were not observed. The gut-associated lymphoid tissue (GALT) was underdeveloped, characterized by the absence of organized lymphoid structures. Nevertheless, diverse populations of diffuse immune cells were present in the lamina propria. Overall, the architecture and tissue organization of the small intestinal wall in *L. catesbeianus* differ significantly from those of mammals, exhibiting a markedly lower degree of complexity.

Although many aspects, including tissue composition of the amphibian immune system have been described in the last decades, most studies have been dedicated to the *Xenopus*, axolotl and giant salamander (Robert & Ohta, 2009; Ruiz & Robert, 2023; Assis *et al.*, 2023). The information of GALT in the frog is still very limited. GALT is composed of both organized lymphoid structures and diffuse immune cells, including lymphoid nodes, aggregated lymphoid nodules, isolated lymphoid follicles, as well as intraepithelial lymphocytes, dendritic cells, macrophages, mast cells and plasma cells within the lamina propria. As the largest lymphoid tissue in the body, GALT recognizes foreign antigens and abnormal antigens in time by ingesting, processing, presenting antigens (Mitchell & Criscitiello, 2020; Mörbe *et al.*, 2021).

GALT is the most common mucosal associated lymphoid tissues (MALT), and exhibits remarkable diversity across vertebrate lineages. In higher vertebrates (aves and mammals), GALT comprises both diffuse immune cells and organized lymphoid structures, such as aggregated lymphoid nodules and isolated lymphoid follicles. In contrast, poikilothermic vertebrates generally lack organized GALT structures. Their GALT is only composed of diffuse immune cells (Rombout *et al.* 2011; Mitchell & Criscitiello, 2020; Stosik *et al.*, 2023). Anyway, GALT is a conserved feature across all vertebrate phylogeny. Present from agnathans to mammals, it manifests in diverse forms — from the typhlosole in lampreys to aggregated lymphoid nodules in mammals. Despite this structural variation, the core function of GALT remains consistent: to concentrate antigens and facilitate their exposure to lymphocytes within the digestive tract (Mitchell & Criscitiello, 2020).

In the present study, the aggregated lymphoid nodules and isolated lymphoid follicles were not observed in the small intestine wall of *L. catesbeianus*. It supports the note

that amphibians lack secondary lymphoid organs except spleen (Robert & Ohta, 2009). Thus, most principal sites for interaction of mature lymphocytes with antigens are in the MALT (Yaparla *et al.*, 2017). Amphibian GALT does include a range of immune cells, which are specialized to their mucosal surfaces (Colombo *et al.*, 2015). In the present study, the immune cell types were present in a diffuse manner in the epithelium and lamina propria. The small intestine lamina propria harbored a variety of immune cells including lymphocytes, macrophages, eosinophils, mast cells, plasma cells and enteroendocrine cells. These immune cell types have various immunological roles, acting as induction sites for antigen sampling and as effector sites for the transport of secretory immunoglobulins (Zhang *et al.*, 2010). Even though the Peyer's patches and lymphoid follicles were absent, small intestine of *L. catesbeianus* had a relatively well-developed mucosal immune barrier since the presence of a variety of immune cells in a diffuse manner in the epithelium and lamina propria. The pattern of diffuse immune cell distribution appears to be evolutionarily conserved, as evidenced by similar observations in the *L. catesbeianus*.

In addition, the shedding extracellular vesicles were observed in the lumen of small intestine in the present study. The shedding extracellular vesicles were very close to the free surface of the villi of enterocytes. In GI, extracellular vesicles are mainly secreted by immune cells and intestinal epithelial cells (Robbins & Morelli, 2014). Abundant researches have convincingly demonstrated that extracellular vesicles are important contributors to the communication between the immune cells (Robbins & Morelli, 2014), microbiota (Al-Nedawi *et al.*, 2015) and intestinal epithelial cells (van Niel *et al.*, 2001). The extracellular vesicles are the main participators in epithelial barrier function in inflamed intestines and wound healing, as well as being important regulators of immune cell recruitment and having immunomodulatory abilities (Vistro *et al.* 2019; Shen *et al.*, 2021).

In the present study, the intestinal mucosal barrier of *L. catesbeianus* was characterized only at the histological level. Molecules associated with intercellular junction complexes - such as claudin and ZO - remain to be identified. The specific immune cell types contributing to the immune barrier also require further confirmation through immunohistochemical staining using cell-specific markers. In addition, functional assays were not conducted, and thus the physiological role of the mucosal barrier warrants further investigation.

## CONCLUSION

The results showed that both muscularis mucosae and muscularis were thin. The intestinal crypts depressions were not observed in the mucosa, and the duodenal submucosal

glands were also not observed in the submucosa. Moreover, mucosal aggregated lymphoid nodules and isolated lymphoid follicles were absent. These results suggested that the general organization of the small intestine wall of *L. catesbeianus* differed considerably from that of mammals. It was distinctly less complex than small intestine wall of the mammals. The enterocytes contained the lysosomes in the cytoplasm. The junctional complexes were frequently observed between epithelial cells. The shedding extracellular vesicles were very close to the free surface of the villi of enterocytes. The mucosa has a well-developed physical barrier in the small intestine of *L. catesbeianus*. In addition, although the mucosa lacked aggregated lymphoid nodules and isolated lymphoid follicles, the immune cell types including lymphocytes, macrophages, eosinophils, mast cells, plasma cells and enteroendocrine cells, were present in a diffuse manner in the epithelium and lamina propria. It is suggested that small intestine of *L. catesbeianus* possessed a relatively low-level GALT, which constitute immune barrier of mucosa. Taken together, the small intestine mucosal barrier is composed of the well-developed physical barrier and relatively elementary immune barrier in the *L. catesbeianus*. Our results demonstrate that *L. catesbeianus* possesses: (i) a structurally reduced but functionally competent physical barrier, and (ii) an immunologically dispersed but cell-type diverse defense system. This configuration likely represents foundational data for comparative studies of mucosal immunity and adaptive innovations for dual aquatic-terrestrial existence.

**YOU, W.; LI, H.; CHEN, H.; ZHAN, X.; LIU, C.; CHEN, S.; YE, Y. & ZHANG, H.** Evidencia histológica de la barrera mucosa en el intestino delgado de la rana toro (*Lithobates catesbeianus*). *Int. J. Morphol.*, 44(1):60-70, 2026.

**RESUMEN:** La mucosa del intestino delgado representa una barrera crucial entre el entorno interno y externo. Si bien la organización de la barrera mucosa intestinal se ha estudiado ampliamente en mamíferos, los datos de vertebrados no mamíferos son limitados. En este trabajo, caracterizamos la organización de la barrera mucosa en el intestino delgado de la rana toro (*Lithobates catesbeianus*) mediante análisis histológicos y ultraestructurales. La investigación histológica mostró que la pared del intestino delgado de *L. catesbeianus* era delgada debido al pequeño número de capas de células musculares lisas en la *muscularis mucosae* (grosor  $1,82 \pm 0,32 \mu\text{m}$ ) y *muscularis* (grosor  $44,95 \pm 3,22 \mu\text{m}$ ). La investigación de microscopía electrónica de transmisión (TEM) mostró los complejos de unión que incluyen uniones estrechas entre enterocitos, y las vesículas extracelulares desprendidas se observaron en estrecha proximidad a la superficie de las microvellosidades en el lumen. Estas estructuras formaron una barrera física junto con las células epiteliales y la capa mucosa. Además, una barrera inmune relativamente elemental estaba compuesta por tipos de células inmunes residentes en la mucosa, incluyendo linfocitos, macrófagos, mastocitos, células plasmáticas, eosinófilos y células enteroendocrinas. En conjunto, la barrera mucosa del intestino delgado de *L. catesbeianus* constaba de dos

partes: la barrera física y la barrera inmunitaria, lo que constituía una barrera mucosa del intestino delgado relativamente bien desarrollada. Estos hallazgos proporcionan datos de referencia para comprender la evolución de la barrera mucosa en vertebrados.

**PALABRAS CLAVE:** Anfibio; Intestino; Ultraestructura; Inmunitario.

## REFERENCES

- Akiba, Y.; Hashimoto, S. & Kaunitz, J. D. Duodenal chemosensory system: Enterocytes, enteroendocrine cells and tuft cells. *Curr. Opin. Gastroenterol.*, 36(6):501-8, 2020.
- Al-Nedawi, K.; Mian, M. F.; Hossain, N.; Karimi, K.; Mao, Y. K.; Forsythe, P.; Min, K. K.; Stanisiz, A. M.; Kunze, W. A. & Bienenstock, J. Gut commensal microvesicles reproduce parent bacterial signals to host immune and enteric nervous systems. *FASEB J.*, 29(2):684-95, 2015.
- An, J.; Liu, Y.; Wang, Y.; Fan, R.; Hu, X.; Zhang, F.; Yang, J. & Chen, J. The role of intestinal mucosal barrier in autoimmune disease: A potential target. *Front. Immunol.*, 13:871713, 2022.
- Assis, V. R.; Robert, J. & Titon, S. C. M. Introduction to the special issue amphibian immunity: Stress, disease and ecoimmunology. *Philos. Trans. R. Soc. Lond. B Biol. Sci.*, 378(1882):20220117, 2023.
- Bizjak Mali, L. & Bulog, B. Histology and ultrastructure of the gut epithelium of the neotenic cave salamander *Proteus anguinus* (Amphibia, Caudata). *J. Morphol.*, 259(1):82-9, 2004.
- Bodegas, M. E.; Villaro, A. C.; Burrell, M. A.; Rovira, J.; Valverde, E.; Ortiz de Zárate, A. & Sesma, P. An immunocytochemical and ultrastructural study of the larval anterior intestine of the frog *Rana temporaria*, with special reference to endocrine cells. *Tissue Cell*, 29(5):545-59, 1997.
- Colombo, B. M.; Scalvenzi, T.; Benlamara, S. & Pollet, N. Microbiota and mucosal immunity in amphibians. *Front. Immunol.*, 6:111, 2015.
- Dwivedy, A. & Aich, P. Importance of innate mucosal immunity and the promises it holds. *Int. J. Gen. Med.*, 4:299-311, 2011.
- Ge, T.; Ye, Y. & Zhang, H. Ultrastructure of telocytes, a new type of interstitial cells in the myocardium of the Chinese giant salamander (*Andrias davidianus*). *Eur. J. Histochem.*, 63(2):3021, 2019.
- Keita, A. V. & Söderholm, J. D. The intestinal barrier and its regulation by neuroimmune factors. *Neurogastroenterol. Motil.*, 22(7):718-33, 2010.
- Mitchell, C. D. & Criscitello, M. F. Comparative study of cartilaginous fish divulges insights into the early evolution of primary, secondary and mucosal lymphoid tissue architecture. *Fish Shellfish Immunol.*, 107 (Pt. B):435-43, 2020.
- Mörbe, U. M.; Jørgensen, P. B.; Fenton, T. M.; von Burg, N.; Riis, L. B.; Spencer, J. & Agace, W. W. Human gut-associated lymphoid tissues (GALT): Diversity, structure and function. *Mucosal Immunol.*, 14(4):793-802, 2021.
- Oliveira, C. P. A.; Carneiro, A. A.; Ervilha, L. O. G.; Machado-Neves, M.; Souza, A. C. F. & Carvalho, R. P. R. Does environmental pollution affect the male reproductive system in naturally exposed vertebrates? A systematic review. *Theriogenology*, 198:305-16, 2023.
- Peterson, L. W. & Artis, D. Intestinal epithelial cells: Regulators of barrier function and immune homeostasis. *Nat. Rev. Immunol.*, 14(3):141-53, 2014.
- Robbins, P. D. & Morelli, A. E. Regulation of immune responses by extracellular vesicles. *Nat. Rev. Immunol.*, 14(3):195-208, 2014.
- Robert, J. & Ohta, Y. Comparative and developmental study of the immune system in *Xenopus*. *Dev. Dyn.*, 238(6):1249-70, 2009.
- Rombout, J. H.; Abelli, L.; Picchiatti, S.; Scapigliati, G. & Kiron, V. Teleost intestinal immunology. *Fish Shellfish Immunol.*, 31(5):616-26, 2011.
- Ruiz, V. L. & Robert, J. The amphibian immune system. *Philos. Trans. R. Soc. Lond. B Biol. Sci.*, 378(1882):20220123, 2023.
- Segatelli, T. M.; Batlouni, S. R. & França, L. R. Duration of spermatogenesis in the bullfrog (*Lithobates catesbeianus*). *Theriogenology*, 72(7):894-901, 2009.

- Shen, Q.; Huang, Z.; Yao, J. & Jin, Y. Extracellular vesicles-mediated interaction within the intestinal microenvironment in inflammatory bowel disease. *J. Adv. Res.*, 37:221-33, 2021.
- Stosik, M.; Tokarz-Deptula, B. & Deptula, W. Immunity of the intestinal mucosa in teleost fish. *Fish Shellfish Immunol.*, 133:108572, 2023.
- Valencia-Aguilar, A.; Ruano-Fajardo, G.; Lambertini, C.; da Silva Leite, D.; Toledo, L. F. & Mott, T. Chytrid fungus acts as a generalist pathogen infecting species-rich amphibian families in Brazilian rainforests. *Dis. Aquat. Organ.*, 114(1):61-7, 2015.
- van Niel, G.; Raposo, G.; Candalh, C.; Boussac, M.; Hershberg, R.; Cerf-Bensussan, N. & Heyman, M. Intestinal epithelial cells secrete exosome-like vesicles. *Gastroenterology*, 121(2):337-49, 2001.
- Yaparla, A.; Koubourli, D. V.; Wendel, E. S. & Grayfer, L. Immune System Organs of Amphibians. *Ref. Modul. Life Sci.*, 1-7, 2017.
- Vistro, W. A.; Huang, Y.; Bai, X.; Yang, P.; Haseeb, A.; Chen, H.; Liu, Y.; Yue, Z.; Tarique, I. & Chen, Q. In vivo multivesicular body and exosome secretion in the intestinal epithelial cells of turtles during hibernation. *Microsc. Microanal.*, 25(6):1341-51, 2019.
- Wang, Z.; Xu, Y.; Huang, L.; Zhao, J.; Ye, Y.; Liu, C.; Wang, B.; Zhao, H. & Zhang, H. Ultrastructural characteristics and morphological relationships of cardiomyocytes and telocytes in the myocardium of the bullfrog (*Rana catesbeiana*). *Anat. Histol. Embryol.*, 53(1):e13008, 2024.
- Zhang, Y. A.; Salinas, I.; Li, J.; Parra, D.; Björk, S.; Xu, Z.; LaPatra, S. E.; Bartholomew, J. & Sunyer, J. O. IgT, a primitive immunoglobulin class specialized in mucosal immunity. *Nat. Immunol.*, 11(9):827-35, 2010.

Corresponding author:

Yaqiong Ye  
College of Animal Science and Technology  
Foshan University  
Foshan  
CHINA

E-mail: cn874462@163.com

Corresponding author:

Hui Zhang  
College of Animal Science and Technology  
Foshan University  
Foshan  
CHINA

E-mail: zhanghui429@hotmail.com